Electronic Supplementary Material (ESI) for Physical Chemistry Chemical Physics.

Molecular Mechanism of Non-covalent Inhibitor WU-04 Targeting SARS-CoV-2 3CLpro and Computational Evaluation of Its Effectiveness Against Mainstream Coronaviruses

Jianhua Wu,[†] Hong-Xing Zhang[†,*] and Jilong Zhang,[†,*]

[†] Institute of Theoretical Chemistry, College of Chemistry, Jilin University, Changchun 130023, Jilin, People's Republic of China.

Table S1. Binding free energy and each energy term of the SARS-CoV-2 bound WU-04 system with two different histidine protonated states were calculated using the MM/GBSA and IE methods (All values given in kcal/mol).

System	Trajectories	ΔE_{vdW}	ΔE_{ele}	ΔG_{gb}	ΔG_{np}	ΔH	$-T\Delta S$	ΔG_{bind}
41(N_δ, HD) + 164(N_ε, HE)	Run_1	-59.40+/-2.52	-43.61+/-5.70	66.56+/-4.56	-5.68+/-0.14	-42.14+/-2.77	9.64+/-2.82	-32.50+/-3.95
	Run_2	-57.71+/-2.59	-40.85+/-5.34	63.80+/-4.13	-5.65+/-0.15	-40.42+/-2.89	10.12+/-1.16	-30.30+/-3.12
	Run_3	-59.44+/-2.64	-45.12+/-5.03	66.23+/-4.10	-5.76+/-0.12	-44.09+/-3.13	10.48+/-1.71	-33.61+/-3.56
	Avg±SD	-58.85+/-0.76	-43.19+/-1.56	65.53+/-1.15	-5.70+/-0.04	-42.22+/-1.25	10.08+/-0.29	-32.14+/-1.22
41(Nε, HE) + 164(Nδ, HD)	Run_1	-59.20+/-2.72	-42.89+/-5.57	66.42+/-4.87	-5.93+/-0.16	-41.61+/-3.05	13.21+/-3.77	-28.40+/-4.86
	Run_2	-56.90+/-3.23	-40.73+/-7.21	62.73+/-6.21	-5.60+/-0.24	-40.50+/-3.39	12.14+/-4.76	-28.36+/-5.84
	Run_3	-56.23+/-3.00	-42.38+/-6.44	63.37+/-5.23	-5.77+/-0.20	-41.02+/-3.17	12.59+/-3.61	-28.43+/-4.81
	Avg±SD	-57.44+/-1.17	-42.00+/-0.85	64.17+/-1.50	-5.77+/-0.11	-41.04+/-0.38	12.65+/-0.38	-28.40+/-0.02

Table S2. Binding free energy and each energy terms of the SARS-CoV-2 and eight mainstream coronaviruses with WU-04 calculated by the MM/GBSA and IE method. All values given in kcal/mol.

System	ΔE_{vdW}	ΔE_{ele}	ΔG_{gb}	ΔG_{np}	ΔH	$-T\Delta S$	ΔG_{bind}
SARS-CoV-2	-58.85	-43.19	65.53	-5.70	-42.22	10.08	-32.14 +/- 1.22
Alpha	-59.55	-50.53	71.39	-5.73	-44.43	15.91	-28.52 +/- 4.12
Beta	-58.51	-40.62	64.37	-5.70	-40.45	10.29	-30.17 +/- 4.14
Gamma	-59.71	-48.06	70.56	-5.74	-42.96	12.53	-30.43 +/- 4.41
Delta	-60.43	-44.39	66.26	-5.80	-44.37	13.86	-30.51 +/- 4.74
Omicron	-59.54	-44.42	67.13	-5.81	-42.64	10.22	-32.42 +/- 3.44
Lambda	-58.07	-47.04	68.48	-5.59	-42.23	13.14	-29.09 +/- 3.76
SARS-CoV	-59.49	-42.26	66.36	-5.74	-41.13	8.77	-32.36 +/- 4.29

MERS-CoV	-57.77	-40.97	62.87	-5.62	-41.49	9.88	-31.61 +/- 3.06

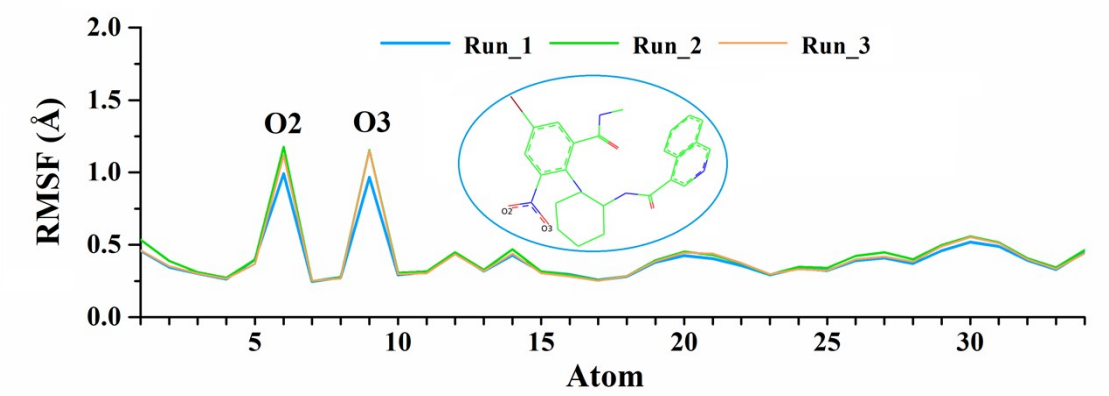

Figure S1. RMSF of the backbone atoms for WU-04. Three repeated MD simulation trajectories of *holo*-3CLpro system are showed and atoms with positional fluctuations near 1 Å are labeled and are shown in black in the figure.

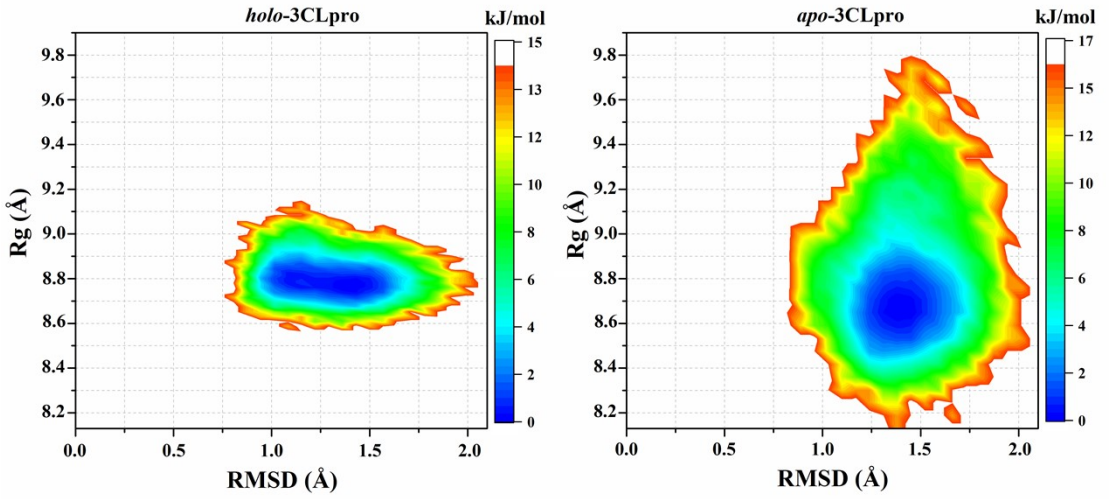

Figure S2. Free energy landscapes as a function of RMSD with Rg values of specific residues near the ligand-binding pocket for the *holo*-3CLpro and *apo*-3CLpro systems.

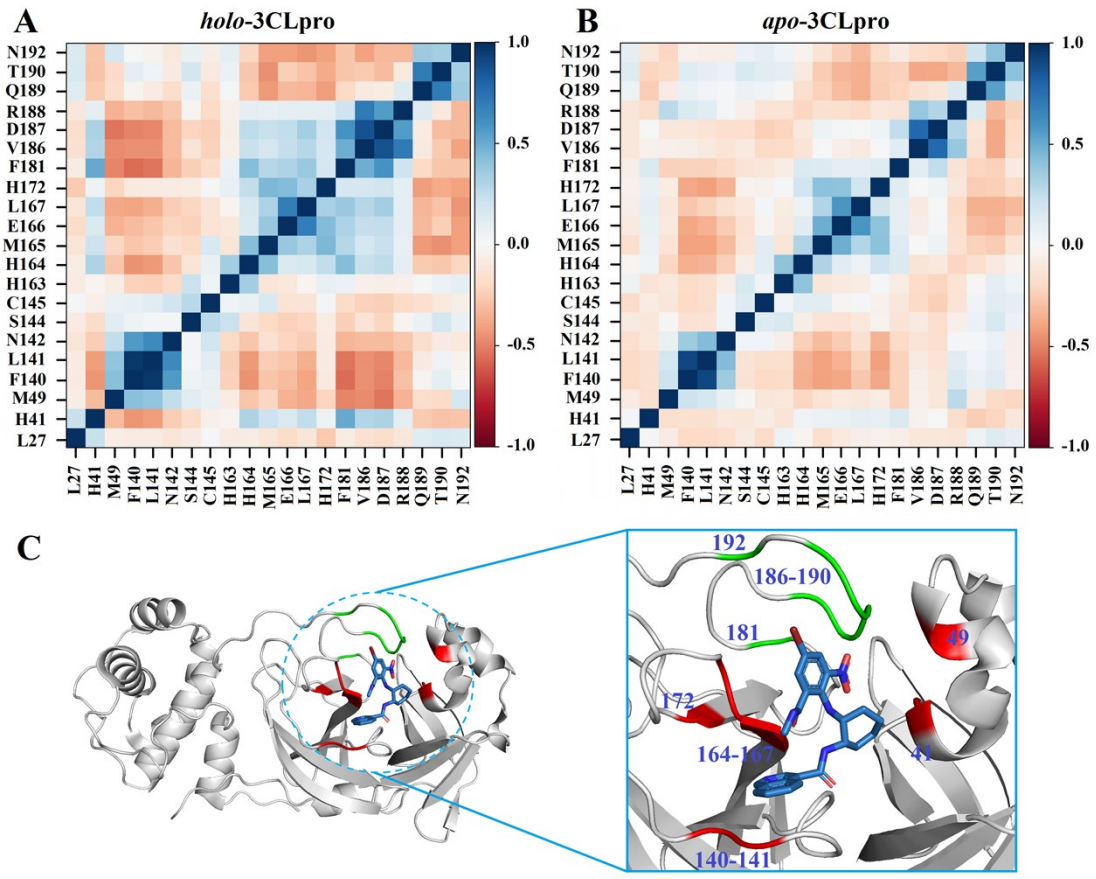

Figure S3. Dynamic cross-correlation maps of residues near the 3CLpro binding pocket for the (A) *holo*-3CLpro and (B) *apo*-3CLpro. (C) Plot of key residues with correlated and anti-correlated motions near the binding pocket.

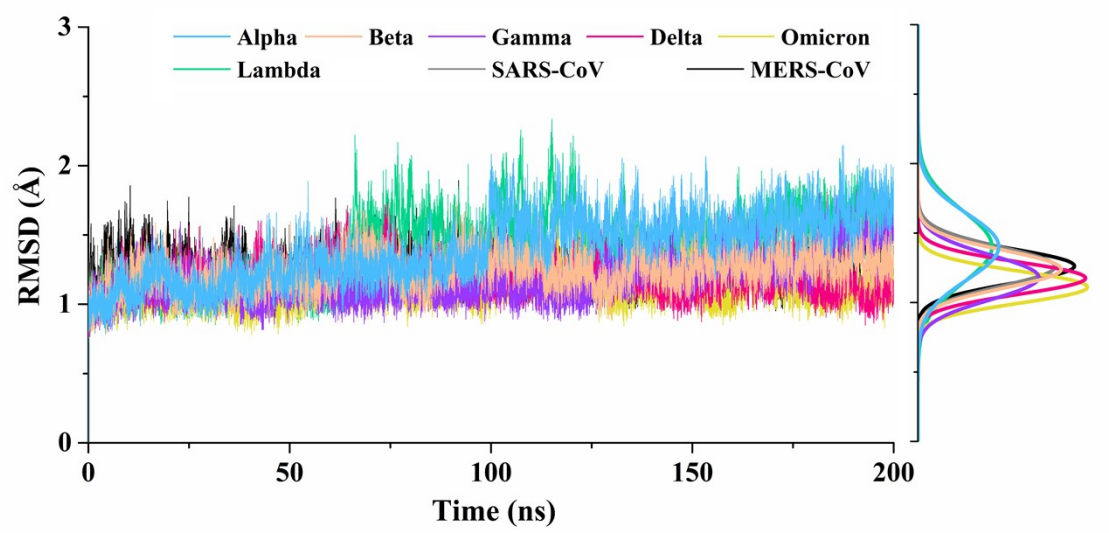

Figure S4. Root mean square deviation (RMSD) of the backbone atoms for the eight mainstream coronavirus Alpha, Beta, Gamma, Delta, Omicron, Lambda, SARS-CoV, and MERS-CoV systems during the MD simulation. The frequencies of the RMSD values for each system are shown on the right of the figure.

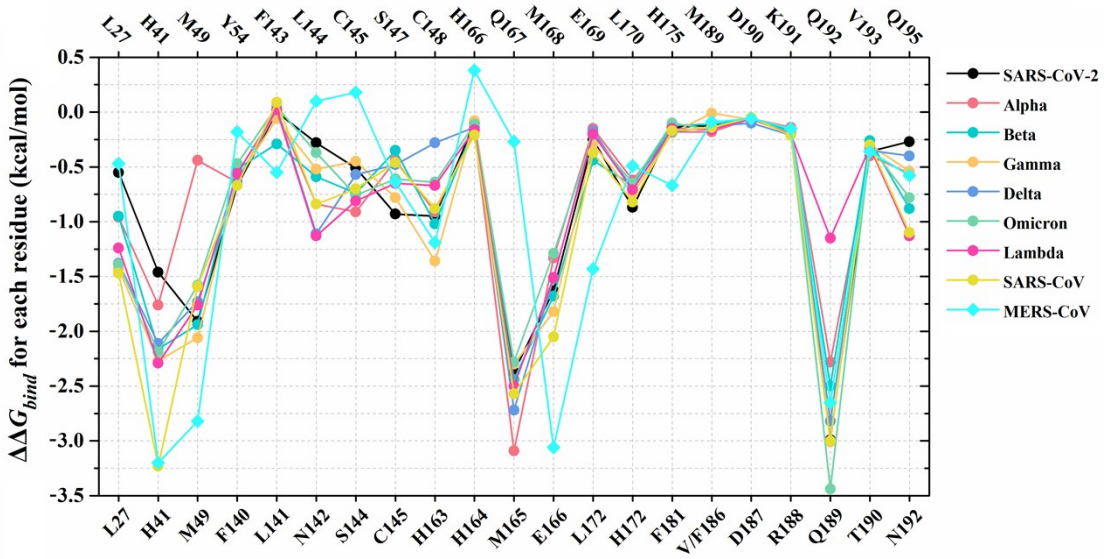

Figure S5. The energy contributions of residues near the binding pocket for SARS-CoV-2 and its six variants and two additional mainstream coronaviruses when interacting with WU-04. As the sequence of the 3CLpro protein of MERS-CoV differs considerably from that of other systems, residues near its binding pocket and their affinity contributions were labeled on the top of the X-axis and shown as diamond (cyan).